Catalysis Today 142 (2009) 152–157

Contents lists available at ScienceDirect

Catalysis Today

journal homepage: www.elsevier.com/locate/cattod

# Role of V in supported V–Sb–O catalysts for the ammoxidation of propane to acrylonitrile: Multilayered $VO_x/SbO_x/Al_2O_3$ catalysts

M. Olga Guerrero-Pérez *, Miguel A. Bañares

*Catalytic Spectroscpy Laboratory, Instituto de Catálisis y Petroleoquímica, CSIC, Marie Curie 2, E-28049 Madrid, Spain*

ARTICLE INFO

*Article history:*
Available online 13 December 2008

*Keywords:*
V–Sb–Al
V–Sb–O
Oxidation
Ammoxidation
Propane
Acrylonitrile
Structure-activity relationship
*In situ* Raman
XRD

ABSTRACT

A synthesis method for multilayered V–Sb–O catalysts on $Al_2O_3$ is described and compared to coimpregnated series; these catalysts are tested for propane ammoxidation. With this preparation method, vanadium and antimony are added sequentially. First, alumina support is impregnated with a loading corresponding to a monolayer of antimony dispersed, it is dried and calcined; then; this solid is impregnated with a vanadium oxide precursor solution. The data obtained are compared with previous papers with catalysts prepared adding both antimony and vanadium at the same time. The new method facilitates the reaction between vanadium and antimony to form the rutile $VSbO_4$ active phase. The presence of dispersed vanadium oxide species along with the rutile $VSbO_4$ phase improves propane conversion.

© 2008 Elsevier B.V. All rights reserved.

## 1. Introduction

Acrylonitrile is widely used as intermediate for the preparation of synthetic rubbers, synthetic resins and fibbers. It is industrially produced nowadays by ammoxidation of propylene on fluid bed reactors with catalysts made of promoted Fe–Bi–Mo–O (BP America) or promoted Fe–Sb–O (Nitto) [1]. Thus, direct conversion of propane into acrylonitrile by ammoxidation of propane is an alternative route to the conventional propylene ammoxidation since propane is substantially cheaper than propylene. More recently, ammoxidation of renewables would be a new route to acrylonitrile formation [2].

There is an important body of research on propane ammoxidation, and the major part of the reported work concentrates on two types of catalysts: the antimonates with rutile structure [3–7] and the molybdates [8–12], both systems usually incorporate vanadium as the key element. Mo–V catalysts modified with niobium and tellurim may afford near 50% yield to acrylonitrile [12] while it reaches 40% on the antimonate system [7,13–14]. Sb–V–O catalysts with an excess of V are highly active and selective for propane oxidative dehydrogenation (ODH) while an excess of Sb affords Sb–V–O catalysts more efficient for propane ammoxidation [15].

Several synthesis methods have been studied for the Sb–V–O based catalysts and it is reported that the synthesis method affects dramatically the activity behavior of catalysts [16]. The most usually studied correspond to patents deposited on 1988 by Standard Oil Co [5–7] and consist on keep a reflux during some hours an aqueous dispersion of $NH_4VO_3$ or $V_2O_5$ and $Sb_2O_3$. Others studies try to keep vanadium as $V^{4+}$ on oxalic acid and then add antimonic acid to this solution [17] or prepare catalysts with a dissolution of $VCl_3$ and $SbCl_5$ on HCl [18], and Brazdil et al. have developed a sol-gel method synthesis for this kind of catalysts [19].

A previous work studied a new synthesis route with Sb–V catalysts supported on alumina [20,21]. With this new method, antimony is added as a soluble tartrate complex. Thus, antimony remains dispersed on the alumina support surface as a monolayer. This work evaluates the relevance on structure, activity and selectivity of sequential vs. simultaneous addition of vanadium and antimony on alumina substrate.

## 2. Experimental and methods

### 2.1. Preparation of samples

Alumina-supported V–Sb–O catalysts were prepared using two procedures. A *two-step process*, where alumina is doped with

* Corresponding author at: Departamento de Ingeniería Química, Universidad de Málaga. Campus de Teatinos, E-29071 Málaga, Spain.
*E-mail address:* oguerrero@uma.es (M. Olga Guerrero-Pérez).

0920-5861/$ – see front matter © 2008 Elsevier B.V. All rights reserved.
doi:10.1016/j.cattod.2008.10.040

antimony, and vanadia is added to $SbO_x/Al_2O_3$, and a *single-step process* in which vanadium and antimony are coimpregnated. The alumina impregnated with antimony (SbTAl) was prepared dissolving the necessary quantity of antimony acetate (Aldrich) on tartaric acid (Sigma) 0.3 M. This solution was stirred until all antimony dissolves; then, γ-$Al_2O_3$ (Versal) was added to the solution. The resulting dissolution was dried in a rotatory evaporator at 80 °C. The resulting solid was dried at 115 °C for 24 h and then calcined at 400 °C for 4 h. SbTAl was prepared so that a total coverage of antimony would correspond to 8 atoms per $nm^2$ of alumina support (this loading would be close to monolayer coverage). Next, the SbTAl modified support was added to an aqueous solution of $NH_4VO_3$ (Sigma) to prepare the vanadium catalysts. The resulting solution was dried in a rotatory evaporator at 80 °C and the resulting solid was dried at 115 °C for 24 h and, finally, calcined at 400 °C for 4 h. This synthesis method is denominated as "*two steps*". This catalyst was prepared so that a total coverage of vanadium would correspond to 25%, 50%, 100% and twice their dispersion limit on the support. This dispersion limit loading, understood as the maximum surface loading of $VO_x$ units that remain dispersed, with no crystalline $V_2O_5$, was determined by Raman spectroscopy to be near 9 $VO_x$ units per $nm^2$ of alumina support, in accordance to previous reports on other supports [22,23]. For the sake of simplicity, these supported catalysts are labeled as "*xV/SbTAl*" where x represent the nominal fraction of dispersion limit ("monolayer" coverage) of V atoms on the support.

For comparative purposes, another series of catalysts is prepared, in which both vanadium and antimony are coimpregnated on alumina support. Alumina is added to a solution containing antimony acetate (Aldrich) dissolved in tartaric acid (Sigma) 0.3 M and $NH_4VO_3$ (Sigma) solutions; this synthesis method is denominated as "*one step*". In a similar fashion to the two-steps series, the resulting solid was dried at 115 °C for 24 h and then calcined at 400 °C for 4 h. The catalysts were prepared so that a total coverage of V + Sb would correspond to the dispersion limit on the alumina support. Three samples were prepared with Sb/V molar ratios of 1, 2 and 4. These supported catalysts are labeled as "1SbyV/Al" where y represents the Sb/V molar ratio.

### 2.2. Characterization

Nitrogen adsorption isotherms (−196 °C) were recorded on an automatic Micromeritics ASAP-2000 apparatus. Prior to the adsorption experiments, samples were outgassed at 413 K for 2 h. BET areas were computed from the adsorption isotherms ($0.05 < P/P_o < 0.27$), taking a value of 0.164 $nm^2$ for the cross-section of the adsorbed $N_2$ molecule at −196 °C. X-ray diffraction patterns were recorded on a Siemens Krystalloflex D-500 diffractometer using Cu K$\alpha$ radiation ($\alpha$ = 0.15418 nm) and a graphite monochromator. Working conditions were 40 kV, 30 mA, and scanning rate of 2°/min for Bragg's angles ($2\theta$) from 5° to 70°. In some cases, the peaks of Al from the sample holder are present.

Raman spectra were run with a single monochromator Renishaw System 1000 equipped with a cooled CCD detector (−73 °C) and holographic super-Notch filter. The holographic Notch filter removes the elastic scattering while the Raman signal remains very high. The samples were excited with the 514 nm Ar line; spectral resolution was ca. 3 $cm^{-1}$ and spectrum acquisition consisted of 20 accumulations of 30 seconds. The spectra were obtained under dehydrated conditions (ca. 120 °C) in a hot stage (Linkam TS-1500). Hydrated samples were obtained at room temperature after and under exposure to a stream of humid synthetic air.

### 2.3. Activity measurements

Activity measurements were performed using a conventional quartz microreactor fitted to an on-line gas chromatograph, equipped with a flame ionization and thermal conductivity detector. The correctness of the analytical determinations was checked for each test by verification that the carbon balance (based on the propane converted) was within the cumulative mean error of the determinations (±10%). To prevent participation of homogeneous reactivity the reactor was designed to minimize gas-phase activation of propane. Tests were made using 0.2 g of sample with particle dimensions in the 0.25–0.125 mm range. The axial temperature profile was monitored by a thermocouple sliding inside a tube inserted into the catalytic bed. Tests were made using the following feedstock: 25% $O_2$, 9.8% propane, 8.6% ammonia in helium. The total flow rate was 20 ml/min corresponding to a gas-space velocity (GHSV) of about 3000 $h^{-1}$. Yields and selectivities in products were determined on the basis of the moles of propane feed and products, considering the number of carbon atoms in each molecule.

## 3. Results

The BET surface areas of the catalyst are listed in the Table 1. The BET area values decrease with surface coverage on $Al_2O_3$ from ca. 265 to 44 $m^2/g$ for the two-step catalyst series. The BET area decrease is less marked for the one-step catalyst series—from 265 to 111 $m^2/g$. For a given vanadium oxide loading, BET area values are higher for the one-step catalyst series.

The XRD patterns of fresh and used catalysts are shown in Fig. 1. Reference samples $Sb_2O_3$, α-$Sb_2O_4$, VSbO4 and $V_2O_5$, were characterized in a previous work [14]. The XRD pattern of the alumina-supported antimony oxide (sample SbTAl) and that of the samples with lower vanadium coverages prepared with the *two-steps* synthesis method (0.25V/SbTAl and 0.5V/SbTAl) exhibit no diffraction pattern, the diffraction pattern of $VSbO_4$ phase (JCPDS file 16-0600) becomes increasingly apparent for 1V/SbTAl and 2V/SbTAl (Fig. 1A) and it grows more intense upon aging in reaction. At the highest vanadium loading, $V_2O_5$ diffraction pattern (JCPDS file 41-1426) is observed for fresh 2V/SbTAl. All aged samples exhibit an increase in the diffraction pattern of $VSbO_4$ phase. The interaction between antimony and vanadium appears promoted during reaction; 0.5V/SbTAl exhibits the features of $VSbO_4$ phase. For 2V/SbTAl, the diffraction pattern of $V_2O_5$ is lost and that of $VSbO_4$ grows stronger. This trend of vanadium to react with antimony during reaction has been described previously [24].

Fig. 1B shows the XRD patterns of the *one-step* series. There are significant differences with the two-step series. The fresh samples generate no diffraction pattern; however, aged 1Sb1V/Al and 1Sb2V/Al exhibit the $VSbO_4$ diffraction pattern. Which is consistent with the trend described above.

**Table 1**
Composition and BET area of alumina-supported Sb–V–O catalysts.

| Catalyst | Synth. Meth. | Sb/V | %Sb | %V | BET area ($m^2/g$) |
|---|---|---|---|---|---|
| $Al_2O_3$ | – | – | – | – | 265 |
| SbTAl | – | – | 29.1 | – | 178 |
| 0.25V/SbTAl | Two steps | 4 | 27.3 | 2.3 | 117 |
| 0.5V/SbTAl | Two steps | 2 | 25.5 | 5.2 | 97 |
| 1V/SbTAl | Two steps | 1 | 22.4 | 11.3 | 66 |
| 2V/SbTAl | Two steps | 0.5 | 18.1 | 18.0 | 44 |
| 1Sb4V/Al | One step | 4 | 13.23 | 1.38 | 114 |
| 1Sb2V/Al | One step | 2 | 11.49 | 2.39 | 111 |
| 1Sb1V/Al | One step | 1 | 9.38 | 3.77 | 139 |

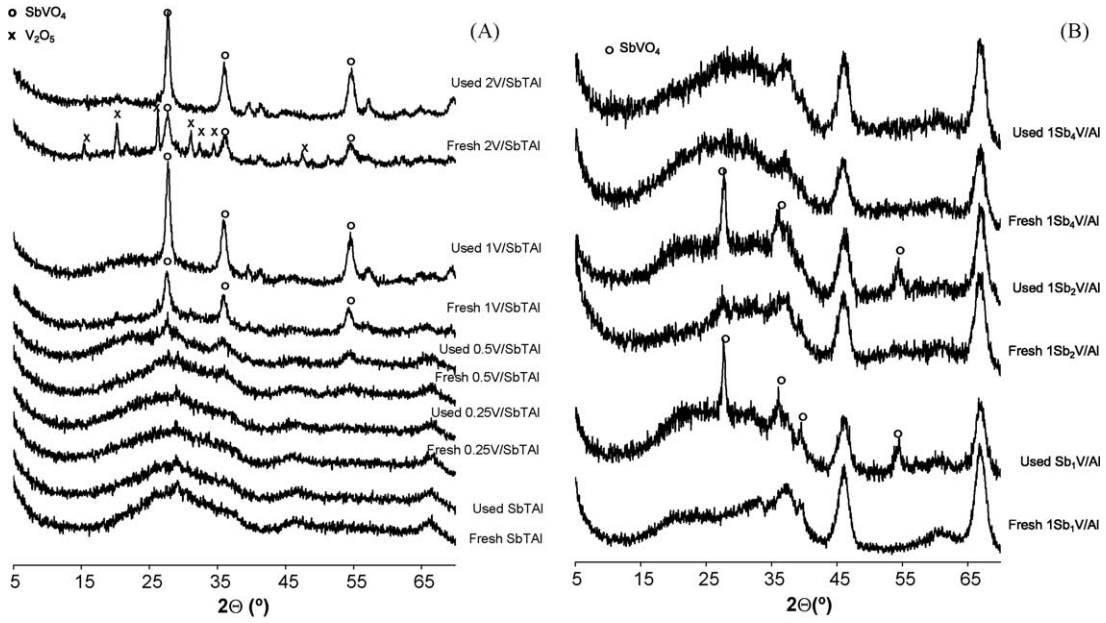


**Fig. 1.** XRD patterns of fresh and used alumina-supported catalysts (A) prepared with the two steps method and (B) with the one step method.

The Raman spectra of dehydrated catalysts are shown in Fig. 2. Reference $Sb_2O_3$ exhibits Raman bands at 190, 255, 372, 451 and 716 $cm^{-1}$; α-$Sb_2O_4$, at 190, 261, 399 and 459 $cm^{-1}$; and $V_2O_5$, at 143, 283, 302, 405, 480, 526, 698 and 994 $cm^{-1}$; finally, $VSbO_4$ exhibits a broad band between 700 and 900 $cm^{-1}$ [14].

Fig. 2A shows the Raman spectrum of alumina impregnated with antimony (SbTAl sample), which posseses weak broad Raman bands at 780, 600, 468 and 210 $cm^{-1}$,corresponding to amorphous antimony oxide [21]. These bands are very weak and can hardly be observed in the presence of stronger vanadium Raman bands. In line with the XRD results, Raman spectra show no bands of crystalline Sb oxides. A weak Raman band near 1024 $cm^{-1}$ in all catalysts is characteristic of the V=O mode of tetrahedral surface $VO_x$ species [23]. This band is affected by hydration, which confirms that it belongs to surface dispersed $VO_x$ species. The Raman spectrum of fresh catalyst with higher vanadium content, 2V/SbTAl, shows Raman bands at 143, 283, 405, 480, 526, 698 and 994 $cm^{-1}$, corresponding to crystalline $V_2O_5$ oxide, in agreement with XRD patterns. The catalysts with vanadium coverage below monolayer, 0.25V/SbTAl and 0.5V/SbTAl exhibit a broad Raman band near 880 and a shoulder near 1000 $cm^{-1}$; these bands belong to bulk Sb–V–O catalysts [15,24], the Raman band near 880 $cm^{-1}$ has been assigned to the $Sb_{0.92}V_{0.92}O_4$ phase [15]. A broad band near 800 $cm^{-1}$ is detected for 1V/SbTAl along with the component at 880 $cm^{-1}$. The Raman band at 800 $cm^{-1}$ appears to be constituted by two Raman bands at 835 and 795 $cm^{-1}$ that have been assigned to the $VSbO_4$ phase [25]; these peaks are well-resolved with UV Raman spectroscopy [26]. The different Raman spectra of V–Sb–O phases have been attributed to the number of Sb vacancies [24]. Raman band corresponding to V–Sb–O in the 700–900 region are not detected in 2V/SbTAl sample because such bands are very weak and $V_2O_5$ oxide is a strong Raman scatter.

Fig. 2B shows the spectra of catalysts prepared with the *one-step* method. The broad Raman band of $VSbO_4$ structure peaks near 800 $cm^{-1}$ and the component near 880 $cm^{-1}$ is hardly visible. Such structure is not visible by XRD, thus, it indicates that $VSbO_4$ crystallites must be present as nanoparticles (NPs), too small to generate a diffraction pattern (up to ca. 4 nm). This series also exhibits the Raman bands of $VO_x$ dispersed species.

Fig. 3 shows the yields to principal reaction products *vs.* reaction temperature for the *one-step* series (alumina impregnated with antimony, SbTAl) and for the two-step series samples 0.25V/SbTAl and 0.5V/SbTAl. The reference catalyst SbTAl, with no vanadium, affords very little propane conversion and $CO_2$ is the

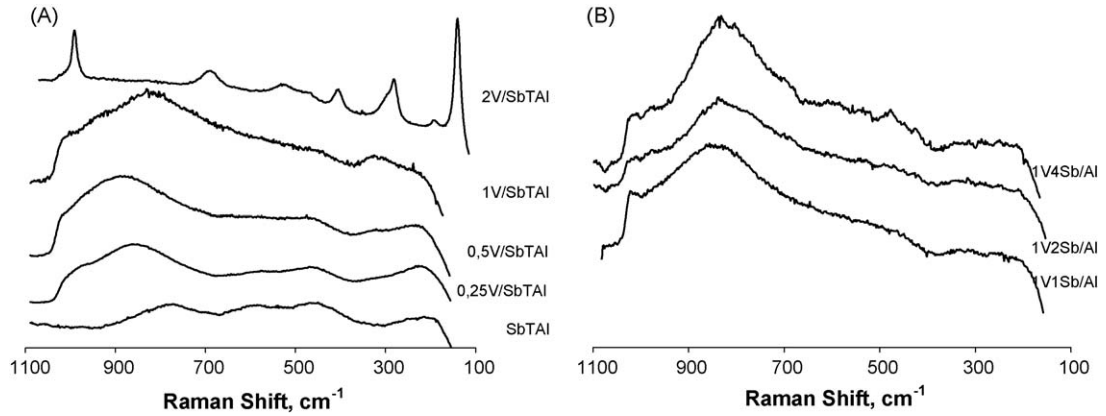


**Fig. 2.** Raman spectra of fresh alumina-supported catalysts (A) prepared with the two steps method and (B) with the one-step method.

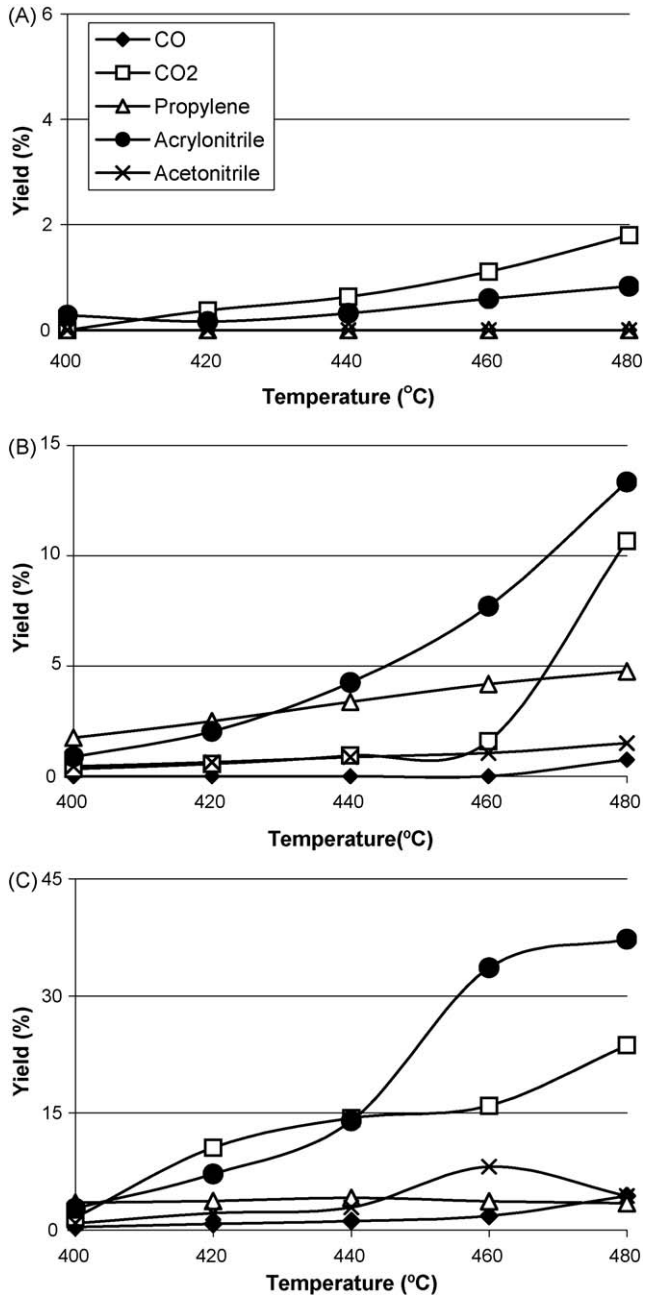


**Fig. 3.** Yields to principal reaction products vs. reaction temperature for (A) SbTAl, (B) 0.25V/SbTAl and (C) 0.5V/SbTAl. Reaction conditions: total flow 20 ml/min; feed composition (% volume): $C_3H_8/O_2/NH_3/He$ (9.8/25/8.6/56.6), 200 mg of catalysts.

main product in the temperature range studied. For 0.25V/SbTAl, acrylonitrile is the main product above 400 °C. With higher vanadium loading, catalyst 0.5V/SbTAl affords significantly higher yields to acrylonitrile above 440 °C. The presence of vanadium makes the alumina-supported antimony oxide much more efficient for propane ammoxidation.

Table 2 shows the results obtained during propane ammoxidation on both catalyst series. Alumina impregnated with antimony, SbTAl, is hardly active and its selectivity to acrylonitrile is 33.6%. Thus, Sb sites possesses the carbon–nitrogen bond formation capability, but total conversion values are remarkably low. The conversion of propane becomes increasingly important with vanadium loading for the two-steps series. However, as the Sb/V atomic ratio decreases, secondary reactions become increasingly important, so that carbon oxides at intermediate Sb/V ratios, and acetonitrile and lower Sb/V ratios compete with acrylonitrile. It should be noted that despite the higher BET are of one-step series catalysts, their activity is lower.

Fig. 4 compares both series for samples with Sb/V = 1, 2 and 4. In both series, propane conversion increases with vanadium content. This is consistent with an optimum performance at Sb/V atomic ratios near 1. Among non-$CO_x$ reaction products, propylene and acrylonitrile exhibit complementary trends, which underlines that propylene is an intermediate in the formation of acrylonitrile. The conversion is higher for the "two-step" preparation series.

## 4. Discussion

The Sb–V–O system is complex; the vanadium antimonite rutiles (JCPDS 16-600, 30-1412, 32-49, 33-122, 35-1485 and 37-1075) generate several diffraction patterns, which correspond to different cell parameters, attributed to non-stoichiometric phases and different synthesis methods. The vanadium antimonate phases are determined by the specific characteristics of the synthesis procedure and by the oxygen partial pressure. For the one-step series, where antimony precursor is molecularly dissolved (tartrate complex); the Raman spectra (Fig. 2B) show the presence of rutile $VSbO_4$ phases. XRD diffraction patterns (Fig. 1B) show that these crystals must be nanoscaled, since no diffraction pattern is generated. However, the XRD patterns of rutile $VSbO_4$ is evident after reaction; thus, $VSbO_4$ crystals grow larger during propane ammoxidation, this is due to the interaction between antimony and vanadium during reaction to form $VSbO_4$ phase [25,27]. From a texbural point of view, the one-step series catalysts exhibit higher surface area values than the "single-step" series.

In the two-step series, vanadium is added in a second synthesis step, and it reacts with antimony forming $VSbO_4$ phases, these aggregates are larger than in the single-step series, since XRD patters show their presence. This reaction appears to take place at the interface with supported antimony oxide, this would allow higher exposure of active sites, making this catalyst series more

**Table 2**
Selectivities and propane conversion values obtained with the alumina-supported catalysts.

| Catalyst | Synthesis steps | Sb/V | Propane conversion (%) | CO selectivity (%) | $CO_2$ selectivity (%) | Propylene selectivity (%) | Acetonitrile selectivity (%) | Acrylonitrile selectivity (%) | Acrylonitrile yield (%) |
|---|---|---|---|---|---|---|---|---|---|
| SbTAl | N/A | – | 1.0 | 0.0 | 66.4 | 0.0 | 0.0 | 33.6 | 0.3 |
| 0.25V/SbTAl | 2 | 4 | 9.4 | 0.0 | 10.0 | 35.8 | 9.1 | 45.1 | 4.2 |
| 0.5V/SbTAl | 2 | 2 | 36.7 | 3.2 | 39.2 | 11.3 | 8.0 | 38.2 | 14.0 |
| 1V/SbTAl | 2 | 1 | 69.8 | 24.5 | 29.1 | 4.7 | 11.4 | 30.3 | 21.1 |
| 2V/SbTAl | 2 | 0.5 | 76.4 | 16.0 | 26.0 | 2.1 | 28.0 | 27.6 | 21.1 |
| 1Sb1V/Al | 1 | 1 | 48.0 | 0.8 | 34.0 | 10.5 | 13.5 | 40.7 | 19.5 |
| 1Sb2V/Al | 1 | 2 | 10.0 | 0.0 | 11.8 | 31.2 | 9.2 | 47.2 | 4.72 |
| 1Sb4V/Al | 1 | 4 | 3.2 | 0.0 | 14.0 | 36.6 | 21.7 | 26.9 | 0.86 |

Reaction conditions: total flow 20 ml/min; feed composition (% volume): $C_3H_8/O_2/NH_3/He$ (9.8/25/8.6/56.6), temperature reaction: 440 °C.

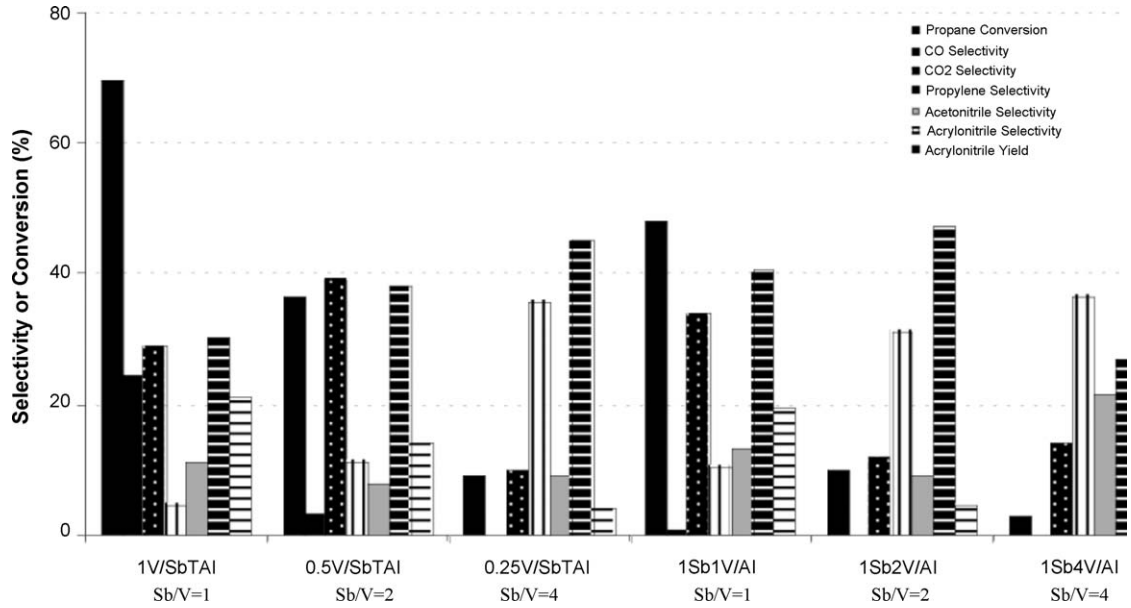


**Fig. 4.** Yields to principal products and propane conversion obtained for catalysts with Sb/V molar ratios of 1, 2 and 4 prepared with both synthesis methods. Reaction conditions: total flow 20 ml/min; feed composition (% volume): $C_3H_8/O_2/NH_3/He$ (9.8/25/8.6/56.6), 200 mg of catalysts, temperature reaction 440 °C.

active. This is consistent with the relevance of exposed vanadium sites to activate propane, as confirmed by operando Raman-GC analyses during ammoxidation reaction [27]. XRD patterns show that the formation of $V_2O_5$ crystalline phase dominates for samples with higher vanadiums content prepared with the two-steps synthesis method; segregated crystalline $V_2O_5$ catalyzes the unselective oxidation of $NH_3$ to $N_2$, lowering acrylonitrile selectivity [6]. Best results are obtained in the absence of vanadium excess. Thus, the two-step procedure would allow a preferential interaction of vanadium with an antimony layer covering alumina. This antimony layer may account for the lower BET are of the two-step series. However, vanadium exposure would be highest for this series, since it would deposit and react on the antimony layer. Thus, the vanadium-antimony reaction would take place close to the surface, and thus the exposure of the $VSbO_4$ phases would be higher. A coimpregnation will result in a more extensive trapping of vanadium ions. Thus, the two-step synthesis procedure allows vanadium species to be added to the antimony-doped alumina, rendering maximum exposure of vanadium sites interacting with antimony; this appears to be critical for propane ammoxidation.

## 5. Conclusions

The performance of vanadium antimonates catalysts is strongly dependent on the interactions between vanadium and antimony. In general, Sb–V–O catalysts are constrained by Sb/V ratio, being active but non-selective for ammoxidation at low Sb/V ratios, and highly selective but not active with antimony excess. This trend is confirmed by the series where both vanadium and antimony are added simultaneously to alumina support. On the other hand, if an antimony-doped alumina is used as a substrate to support vanadium oxide, the scenario becomes different. It is possible to afford signifincatly higher conversion and selectivity values for propane ammoxidation to acrylonitrile. In this series, the vanadium species react with the antimony sites forming vanadium antimonates. Since the alumina support is covered by antimony oxide, all vanadium species are located as lattice species in the rutile vanadium antimonates, or as surface vanadium species on antimony. Both species are involved in the catalytic cycle for the ammoxidation of propane to acrylonitrile [27]; however, the exposure if vanadium sites is critical for propane activiation. The relevance of vanadium exposure accounts for the higher activity, selectivity and tolerance to higher Sb/V ratios in the series where vanadium oxide is added to an antimony-decorated alumina (two-step series).

## Acknowledgments

This research was funded by Ministry of Science and Technology of Spain under project CTQ2005-02802/PPQ. M.O.G.-P. thanks CSIC for an I3PDR-8-02 postdoctoral position. The authors thank Dr. M.A. Vicente from Salamanca University for his help with the XRD analysis and his helpful discussions.

## References

[1] R.K. Grasselli, in: Ertl, et al. (Eds.), Handbook in Catalysis, vol. V, Willey–VCH, 1997, p. 2302.
[2] M.O. Guerrero-Pérez, M.A. Bañares, ChemSusChem 1 (6) (2008) 511.
[3] G. Centi, F. Marchi, S. Perathoner, Appl. Catal. A 149 (1997) 225.
[4] M.O. Guerrero-Pérez, M.V. Martínez-Huerta, J.L.G. Fierro, M.A. Bañares, Appl. Catal. A 298 (2006) 1.
[5] A.T. Guttmann, R.K. Grasselli, J.F. Brazdil, 047949[US4788317] (1988).
[6] L.C. Glaeser, J.F. Brazdil, 887478[US4788173] (1988).
[7] A.T. Guttmann, R.K. Grasselli, J.F. Brazdil, F. 724226[US4746641] (1988).
[8] Y.C. Kim, W. Ueda, Y. Morooka, Catal. Today 13 (1992) 673.
[9] S.I. Woo, J.S. Kim, Stud. Surf. Sci. Catal. 92 (1995) 191.
[10] J.S. Kim, S.I. Woo, Appl. Catal. A 110 (1994) 207.
[11] M.O. Guerrero-Pérez, J.N. Al-Saeedi, V.V. Guliants, M.A. Bañares, Appl. Catal. 260 (1) (2004) 93.
[12] T. Ushikubo, K. Oshima, A. Kayou, M. Hatano, Stud. Surf. Sci. Catal. 112 (1997) 473.
[13] M.O. Guerrero-Pérez, J.L.G. Fierro, M.A. Bañares, Catal. Today 118 (2006) 366.
[14] M.O. Guerrero-Pérez, J.L.G. Fierro, M.A. Vicente, M.A. Bañares, J. Catal. 206 (2002) 339.
[15] R. Nilsson, T. Lindblad, A. Andersson, J. Catal. 148 (1994) 501.
[16] G. Centi, P. Mazzoli, S. Perathoner, Appl. Catal. A 165 (1997) 273.
[17] S.B. Derouane-Abd Hamid, G. Centi, P. Pal, E. Derouane, Top. Catal. 15 (2001) 161.
[18] G. Centi, F. Marchi, Stud. Surf. Sci. Catal. 101 (1996) 277.
[19] J.F. Brazdil, M.A. Toft, J.P. Bartek, R.G. Teller, R.M. Cyngier, Chem. Mater. 10 (1998) 4100.
[20] M.O. Guerrero-Pérez, M.A. Bañares, Catal. Today 96 (4) (2004) 265.
[21] M.O. Guerrero-Pérez, J.L.G. Fierro, M.A. Bañares, Top. Catal. 41 (2006) 43.

[22] I.E. Wachs, L.E. Brian, J.-M. Jehng, L. Burcham, X. Gao, Catal. Today 57 (2000) 323.
[23] M.A. Bañares, I.E. Wachs, J. Raman Spectrosc. 33 (2002) 359.
[24] M.O. Guerrero-Pérez, J.L.G. Fierro, M.A. Vicente, M.A. Bañares, Chem. Mater. 19 (2007) 6621.
[25] M.O. Guerrero-Pérez, M.A. Bañares, Chem. Commun. 12 (2002) 1292.
[26] G. Xiong, V.S. Sullivan, P.C. Stair, G.W. Zajac, S.S. Trail, J.A. Kaduk, J.T. Golab, J.F. Brazdil, J. Catal. 230 (2005) 317.
[27] M.O. Guerrero-Pérez, M.A. Bañares, J. Phys. Chem. C 111 (2007) 1315.